ACADEMIC PRESS

Available online at www.sciencedirect.com

SCIENCE DIRECT®

Journal of Magnetic Resonance 162 (2003) 198–205

JMR Journal of Magnetic Resonance

www.elsevier.com/locate/jmr

Self- and mutual-diffusion coefficients measurements by ^{31}P NMR 1D profiling and PFG-SE in dextran gels

Sungjong Kwak, Minh Tan Phan Viet, and Michel Lafleur*

Département de chimie and Groupe de Recherche en Transport Membranaire, Université de Montréal, C.P. 6128, succursale Centre-ville, Montréal, Qué., Canada H3C 3J7

Received 3 September 2002; revised 30 January 2003

Abstract

^{31}P NMR 1D profiling was successfully introduced to measure macroscale mutual-diffusion coefficients (D_m) of phosphate ions in dextran gels. Series of 1D profiles describing the phosphate concentration along cylindrical dextran gels were acquired at different times. These profiles that included over 600 points could be fitted using equations derived from Fick's law, with D_m as the single fitting parameter. Release and penetration profiles were recorded providing two alternative approaches for allowing the determination of D_m. The D_m values were compared with microscale self-diffusion coefficients (D_s) measured by pulsed field gradient spin echo (PFG-SE) technique. D_m values, measured between 25 and 45 °C, were systematically lower than D_s. The experimental diffusion time and the associated diffusion length of D_s (60 ms, 10 μm) are short compared to those of D_m (up to 18 h, 50 mm). These scale differences are considered to be the origin of different D_s and D_m and provide information relative to the network in these gels.

Keywords: ^{31}P NMR 1D profiling; PFG-SE NMR; Self-diffusion; Mutual-diffusion; Dextran gels

1. Introduction

The diffusion of analytes in hydrogels is a critical parameter that requires a detailed investigation for several systems including drug-trapping hydrogels used as novel controlled-release devices, and gels used for cell immobilization to provide bioreactors. Moreover, transport properties constitute an indirect approach to obtain structural information on gels. In our group, we are especially interested by the diffusion of molecular species in hydrogels to provide a better understanding of solute diffusion in bacterial biofilms. When bacteria attach to surfaces, they are often found embedded in a matrix formed of a polysaccharide gel, living as a microsociety and giving rise to organizations that are referred to as biofilms [1–3]. In biofilms, the diffusion of molecules from or to bacteria is seriously modified [4–6]. However, nutrients must penetrate the biofilms and metabolic waste should be evacuated. Biofilms can display a dramatical increase in antibiotic resistance, and one of the putative explanations is related to the decreased transport rate of the antibiotic agents into the biofilms [7–9]. Therefore, it is essential to obtain a detailed description of the molecular diffusion in this type of matrices to understand the functioning of bacteria within biofilms as well as to determine the source of the bacterial resistance.

Dextran is a polysaccharide that is found in bacterial biofilms [3,10]. It was used in the present study as a crude model for biofilm matrixes to optimize the NMR techniques used to gain insights into molecular diffusion. Dextran is a homopolysaccharide with α-1, 6-linked D-glucose units. Side chains are often formed with α-1, 3 and α-1, 4 interconnections. Thermo-reversible dextran gels are formed when K^+ ions are added to aqueous dextran solutions [11]. The dextran sol–gel transition is considered as a structural change from a random coil polymer to an infinite polymeric network. Using a ^{1}H NMR stimulated-echo method, Watanabe et al. [12] studied the water self-diffusion in dextran gels to examine the structure of the gels. They concluded that K^+ ions induce cross-linking of the polysaccharide chains,

* Corresponding author. Fax: +514-343-7586.
E-mail address: michel.lafleur@UMontreal.ca (M. Lafleur).

1090-7807/03/$ - see front matter © 2003 Elsevier Science (USA). All rights reserved.
doi:10.1016/S1090-7807(03)00047-8

and organize these gels into two regions: pores filled with water molecules relatively free to diffuse, and barriers formed by aggregated polysaccharide chains.

Stimulated-echo and pulsed-field gradient-spin echo (PFG-SE) NMR methods have been used extensively to measure self-diffusion coefficients of solutes in various media [13,14]. The approach is nondestructive and multinuclear experiments can be easily performed on homogeneous samples. Typical diffusion times of PFG-SE NMR experiments are tens of milliseconds. Small solutes with self-diffusion coefficients in the order of $10^{-9}\,m^2/s$ or less travel several microns during this diffusion time. These spatial and temporal characteristics of the methods are fundamental as they define the scale over which the diffusion is sampled. In porous media or gels, inhomogeneities such as pores and barriers are not necessarily probed over this length scale, and the diffusion of molecular species in a gel is not fully described on the sole basis of self-diffusion as the solutes move forward by overcoming barriers, moving from one pore to the others at certain rate, and diffusing within pores.

NMR imaging is an alternative and complementary approach examining the macroscale diffusion of molecules. This method has provided for example the description of macroscopic diffusion in porous media, and solvent uptake by polymers [15–20]. Diffusion times associated to NMR imaging can be hours, and several centimeters of the samples can be probed. Therefore, the time and spatial scales are typically more than 1000 times larger than those of self-diffusion measurements. Recently, Duval et al. [15] used PFG-SE technique and 1D ^{1}H NMR imaging to measure the microscale and macroscale diffusions of water in colloidal gels and showed that their comparison revealed structural information relative to the gels.

In the present study, we have investigated the diffusion of phosphate ions, an essential nutrient for bacteria, in dextran gels, combining PFG-SE techniques and 1D ^{31}P NMR imaging. We have designed three different types of profiling experiments as illustrated in Fig. 1. The bottom of a NMR tube was filled with dextran gel, and the space above was used as a small reservoir. The approach **I** was a release experiment: a gel containing phosphate ions was in contact with a phosphate-free buffer, and phosphate profiles in the gel were recorded as phosphate ions were released out from the gel as a function of time. The approaches **II** and **III** were penetration experiments: phosphate ions from the solution diffuse into phosphate-free dextran gels, and phosphate profiles of the gels were recorded as phosphate ions penetrated in the gels as a function of time. For the approaches **I** and **II**, the small reservoir was connected to the large reservoir outside the magnet to ensure that the phosphate concentration of the solution above the gel was constant over the whole experiments. Only the small reservoir was used for type **III** experiments (see Section 2 for the details). These experiments were a novel approach to extract the mutual-diffusion coefficient (D_m) of phosphate ions using ^{31}P NMR-derived release and penetration profiles. The D_m and D_s values, obtained with 1D profiles and PFG-SE ^{31}P NMR method, respectively, were compared.

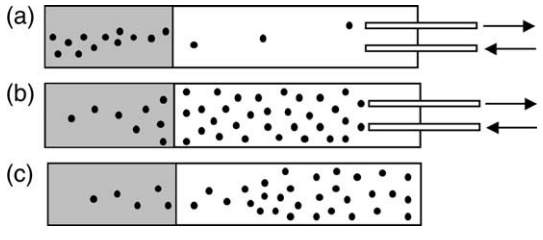

Fig. 1. Schematics of the three types of 1D ^{31}P NMR profiling experiments: (a) type **I**, release experiment; (b, c) type **II** and **III**, penetration experiment with and without large reservoir, respectively. Dextran gels are represented in gray, whereas white areas and small dots represent solutions and phosphate ions, respectively.

2. Experimental

2.1. Sample preparation

Dextran with an average molecular weight of approximately 40,000 was obtained from Sigma (St. Louis, MO) and used as received. In order to prepare 20% dextran gel samples, 1 g of dextran powder was added to a vial containing 4 g of an aqueous solution containing KH_2PO_4 (0.4 M), and KCl (2.1 M), in case of type **I** experiment, or containing only KCl (2.5 M) in case of type **II** and **III** experiments. The K^+ concentration, the gelifying ion, was kept at 2.5 M for all the experiments. The vial was placed in a hot water bath at about 90 °C, and the mixture was stirred vigorously until it became a homogeneous and transparent solution. The vials were sealed carefully with screw caps to prevent the loss of water during the incubation. The solutions were transferred into 10 mm NMR tubes, and became gels as the solutions cooled down to room temperature [12]. NMR experiments were performed at least two days after the sample preparation. The pH of the $KH_2PO_4/KCl/H_2O$ solution was 3.8 and decreased to 3.7 after the addition of dextran powder.

2.2. NMR experiments

The NMR experiments were carried on a Bruker DSX-300 NMR spectrometer operating at 120 MHz for ^{31}P. A Bruker magnetic resonance imaging probe, Micro 2.5 probe, was used in conjunction with a gradient amplifier (BAFPA-40). Gradient pulses were applied along the z-direction, i.e., along the sample tube. The gradient strength was calibrated with one-dimensional

(1D) image profile along the z-axis of a well-defined solid object in water solution containing traces of $CuSO_4$.

2.3. 1D ^{31}P NMR profiling

1D ^{31}P NMR profiling was obtained from a spin-echo sequence with the echo time of 6 ms [21]. The 90° pulse and gradient pulse length were 22 μs and 5.6 ms, respectively, whereas the gradient strength was 6.16 G/cm. The intensity of the profile at each point on the spectrum was considered to be proportional to the phosphorus concentration at corresponding position in the sample tube. T_2 of phosphorus was found slightly dependent on the concentration of the KH_2PO_4. T_2 of phosphate in gels containing 0.05 and 0.4 M phosphate were 118 and 71.5 ms, respectively. Because of the short τ value, this difference in spin–spin relaxation has only a limited influence on the signal intensity. The relative intensity in the concentrated region of the profile was reduced by about 6% compared to that in the diluted region. This difference associated to a T_2 effect hardly affects the calculation of the D_m. Relaxation delay was 2.5 s ($T1 \cong 0.5$ s), and 500 scans were co-added for each profile, leading to an acquisition time of about 20 min. The field of view was 50 mm, and 512 data points were acquired with a 50–125 Hz (about 400 ppm) spectral window. Therefore, the digital resolution of these experiments was 97 μm per point.

Dextran gels filled the bottom of the NMR tubes, and the space above was used as a small reservoir (~7 ml). The reservoir is filled with a 2.5 M KCl/H_2O solution or a 0.4 M KH_2PO_4/2.1 M KCl/H_2O solution depending on the type of the experiments. The KCl solution was used to maintain the K^+ concentration constant, a prerequisite to prevent the degradation of the gels. For phosphate release experiments (approach **I**), dextran gels containing phosphate ion were used with phosphate-free solutions. The small reservoir was connected with a large reservoir (500 ml) located outside the magnet. The solution circulation between the small and large reservoirs was ensured by a peristaltic pump (Master-Flex), with a flow rate between 1.5 and 2 ml/min. Using this set-up, the phosphate concentration at the gel/water interface was kept constant at zero through out the experiment. The first ^{31}P profile was recorded immediately after the addition of the potassium chloride solution in the tube, and subsequently profiles were recorded every 3 h for at least 18 h.

For phosphate ion-penetration experiments (types **II** and **III**), dextran gels without phosphate ion were put in contact with phosphate ion-containing solutions in the reservoir. The recording of the profiles was performed similarly to that for the release experiments. For the approach **III**, only the small reservoir was used to determine whether such simplified set-up was sufficient to ensure that the phosphate concentration decrease near the gel–reservoir interface was negligible, a requisite condition for the profile analysis.

2.4. 1D profile data processing

The 1D profiling experiments were designed to meet the conditions of the equations developed for the diffusion in semi-infinite media by Crank [22]. For type **I** release experiments, the dextran gel is considered as a semi-infinite medium, whose surface is maintained at a zero concentration. At time equal 0, the phosphate concentration through out the gel is C_0. As the diffusion proceeds, phosphate ions are released from the gel, and the concentration dependence on the distance from the gel/water interface, defined as $x = 0$, is given by the following equation:

$$C/C_0 = \mathrm{erf}[x/2(D_m t)^{1/2}], \tag{1}$$

where C is the concentration at a distance x from the interface at an elapsed time t, and D_m is the mutual-diffusion coefficient. In case of the experiments of types **II** and **III**, the phosphate diffusion occurs in an opposite direction, i.e., from the reservoir to the gel. The concentration at the interface is maintained constant at C_0' through out the experiment, and the initial concentration in the gel is zero. Eq. (2) describes the expected concentration profiles under these conditions:

$$C/C_0' = \mathrm{erfc}[x/2(D_m t)^{1/2}]. \tag{2}$$

In order to calculate D_m, baseline corrected profiles were normalized to C_0 or C_0' depending on the type of experiments. For the release experiments, each profile was divided by the profile obtained at time zero as the intensity is representative of C_0. For the penetration experiments, the profiles were divided by the intensity measured at the interface at time equal 0 because it is representative of C_0'. Subsequently, all the profiles acquired at different elapsed times for a given experiment were fitted simultaneously with the appropriate equation to determine a single least-square fitted D_m value. The results were reproducible within 5%. The nonlinear least-square fitting routine in Microcal Origin (version 5.0) was used.

2.5. Self-diffusion coefficient measurements

The Stejskal–Tanner PFG-SE pulse sequence was used [23]. Self-diffusion measurements were done by increasing gradient field strength, G, from 5 to 80 G/cm, and the other parameters were kept constant; the 90° pulse length (22 μs), the gradient pulse length ($\delta = 2.5$–3.0 ms), and the delay between the two gradient pulses ($\Delta = 60$ ms) were those indicated in parentheses. After Fourier transform, absolute value calculation was done to eliminate phase disturbance of multiplets caused

by homonuclear spin–spin coupling, and the integral of the resonance peaks were used for the diffusion coefficient determination. In order to compare self- and mutual-diffusion coefficients of each sample, self-diffusion measurements were carried out before 1D profiling for type **I** experiments. In case of penetration experiments (approaches **II** and **III**), self-diffusion measurements were done more than four weeks after the 1D ^{31}P NMR profiling, in order to get a relatively homogeneous phosphate concentration in the gel. The experimental incertainty on D_s measurements was estimated to be 5% or less.

3. Results

Fig. 2a shows typical 1D ^{31}P NMR profiles of phosphate ion release from 20% dextran gels at 37 °C (approach **I**). For the sake of clarity, only 5 out of the 7 recorded profiles are displayed. Profile 1 was recorded at time equal 0. The interface is clearly observed at about pixel number 50 by the sharp decrease in the phosphorus signal, the gel being located in the space displayed on the left side of the graph. The anomalous slight increase in intensity near the interface was a reproducible feature and is considered to be due to the inhomogeneity of the magnetic susceptibility at the boundary of the gel and the solution. At the beginning of the experiment, the phosphate concentration should be constant through out the gel. However, the intensity decreases progressively to nothing on the left side of the profile (pixel numbers 250–350). This is mainly attributed to the inhomogeneity of the radio pulses along z-axis. Nevertheless, a region near the center of the profile shows a rather constant intensity and only this part of the raw profiles, delimited by the two dashed lines in Fig. 2a, is subsequently used for the D_m calculation (Fig. 2b). Over the course of the experiments, the dextran gels did not show any swelling and, therefore, the location of the interface between gel and solution is kept at fixed position on the 1D profiles.

As phosphate ions are released from the gel, the intensity of the signal decreases from near the interface, and this decrease becomes more pronounced as a function of time. As can be seen on the profiles, the phosphate concentration practically remains nil in the solution (pixel number 0–50), indicating the efficiency of our set-up. The averaged intensity of this section of the profile is considered as a baseline. The baseline corrected profiles are normalized relative to C_0 (profile 1). The exact position of the interface is defined as the pixel where the profiles reach a zero intensity, and the x-axis is converted into distance as described in the experimental section. Subsequently, all six profiles are simultaneously fitted with Eq. (1), sharing a single fitted value of D_m. The least-square fitted curves are displayed in Fig. 2b. Each profile contains over 100 points, so, more than 600 points are fitted at the same time to determine the D_m value. The experimental profiles are well fitted with Eq. (1), indicating a Fick-type diffusion. The D_m values are reported in Table 1.

Fig. 3a shows the raw 1D profiles for the penetration experiment (approach **II**). On profile 1, the interface is observed at about pixel number 160, from the abrupt increase in the phosphorus intensity. The phosphate-free gel corresponds to the left side of the figure. Similar to the release profiles, the experiment conditions (rf pulse) were homogeneous over a section of the profiles. In the solution (right of the interface), the phosphate concentration should be constant whereas a decrease in signal intensity is observed at the end of the profile (pixel number >200). The region indicated by the two dashed lines is considered for D_m calculations. Over the course of the experiments, the signal intensity in the gel

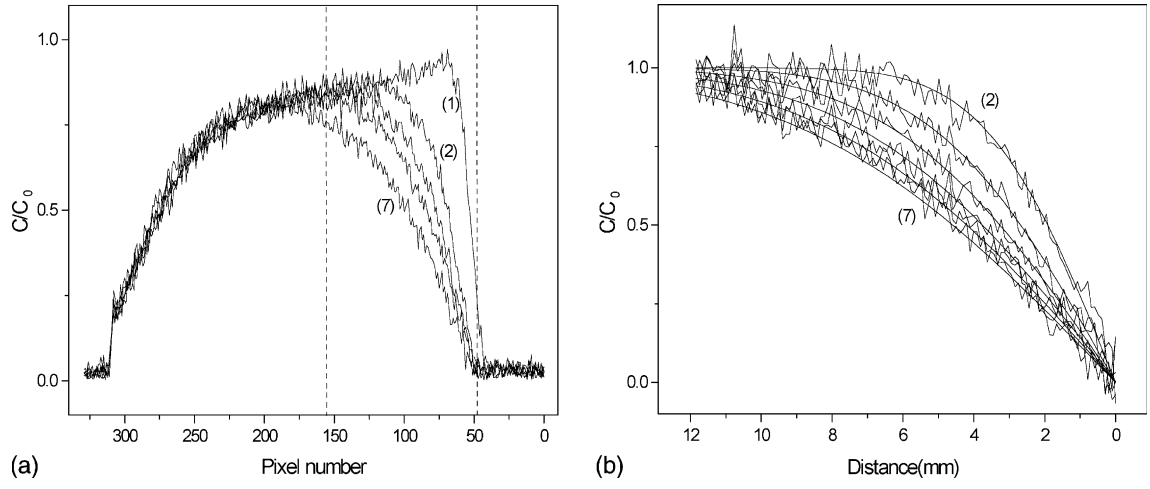

Fig. 2. (a) Raw 1D ^{31}P NMR profiles obtained from phosphate release experiments (type **I**) and (b) the normalized profiles and the least-squares fitted curves.

Table 1
Mutual- and self-diffusion coefficients ($\times 10^{10}\,m^2/s$) of phosphate ion in 20% dextran/H_2O gel

T (°C)	Type	D_m	D_s
25	I	2.2	2.6
	II	1.3	2.8
	III	1.2	2.7
	Free in solution		8.0
37	I	3.5	4.1
	II	1.8	4.0
	III	1.7	3.9
45	I	4.1	4.9
	II	2.3	4.9
	III	2.2	4.9

increases progressively. In addition, it can be observed that the signal intensity and therefore the phosphate concentration remain constant at the interface. The profiles are normalized with the phosphate interfacial concentration, using the maximum intensity of the profiles, and the x-axis is converted into distance. The profiles are then simultaneously fitted with Eq. (2) to obtain the D_m value that is reported in Table 1. In this case again, the model successfully reproduces all the profiles, which include over 600 experimental points.

Table 1 and Fig. 4 summarize the diffusion coefficients measured with the different approaches at 25, 37, and 45 °C. Self-diffusion measurements of phosphate in aqueous solutions were also carried out for the comparison, and D_s of phosphate ions in an aqueous KCl solution (2.5 M), at 25 °C, is found to be $8.0 \times 10^{-10}\,m^2/s$, in good agreement with previously reported data [24]. This comparison clearly shows that the diffusion of phosphate in dextran gels is hindered relative to that in aqueous solutions. For the release experiments (approach **I**), D_s was measured prior to the recording of the release profiles. Penetration experiments (approaches **II** and **III**) were performed with phosphate-free gels. As a consequence, D_s were obtained after an extensive incubation with the phosphate solution. The various D_s values measured for a given system are the same within the range of the experimental error. The self-diffusion measurements at 25 °C were also performed with a delay between the two gradient pulses (Δ) varying between 20 and 400 ms. No significant differences in D_s were observed (data not shown). D_m values are systematically lower than D_s, and D_m from release (approach I) and penetration profiles (approaches II and III) are significantly different from each other.

The penetration experiments were performed using a large reservoir (approach **II**) and using only the upper part of the NMR tube as a small solution reservoir (approach **III**), a simplified set-up compared to the approach **II**. Despite the limited volume of the reservoir, the penetration profiles in these cases were similar with those obtained with the approach **II** experiments. The purpose of using a large reservoir was to maintain the phosphate ion concentration at the interface constant through out the experiments. However, the results indicate that the fast phosphate ion diffusion in solution is enough to compensate phosphate ion loss at the interface generated by the ion penetration. D_s of phosphate ion in solution is about 6-fold faster than that obtained from the penetration experiments at the same temperature. This faster diffusion ensures a constant interfacial phosphate concentration over the period of the experiments. Typically, profiles were acquired over 18 h and during this period, about 4–5% of the phosphate in the solution reservoir diffused into the gel. This change in phosphate concentration of the reservoir has no significant impact. Consequently, it appears that the more sophisticated set-up that includes an additional large reservoir and a pump system is not absolutely required for the penetration experiments.

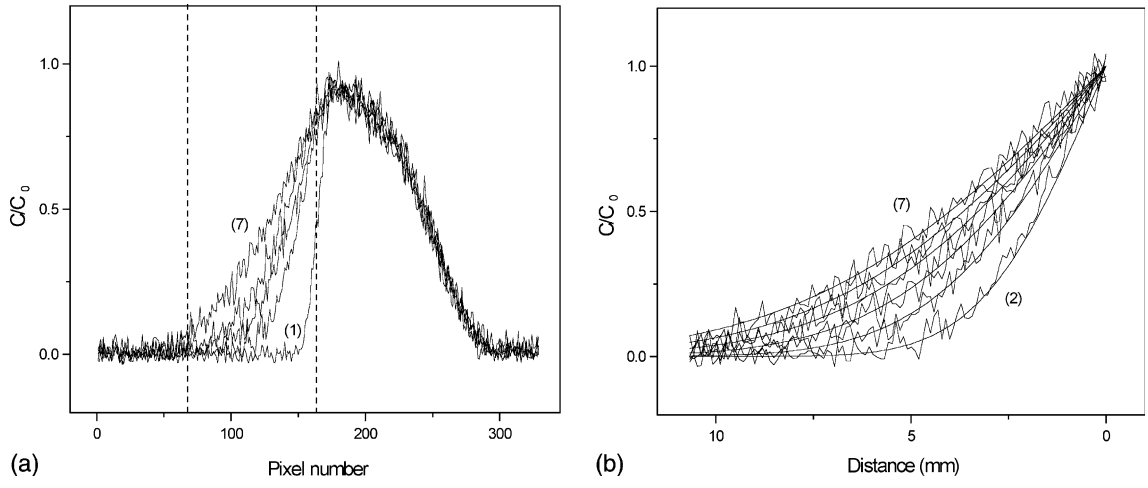

Fig. 3. (a) Raw 1D ^{31}P NMR profiles obtained from phosphate penetration experiments (type **II**) and (b) the normalized profiles and the least-squares fitted curves.

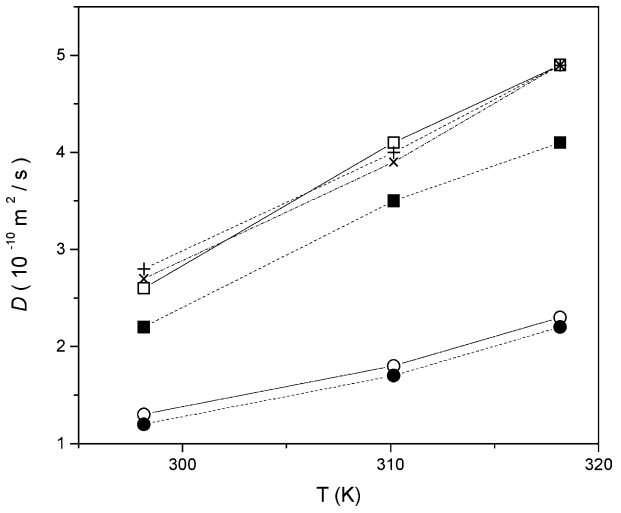

Fig. 4. Evolution as a function of temperature of the self- and mutual-diffusion coefficients ($10^{-10}\,m^2/s$) of the phosphate ions in dextran gels. D_s obtained from gels used in release (□), and penetration (types **II** (+) and **III** (×)) experiments. D_m extracted from release (■), and penetration (types **II** (○) and **III** (●)) experiments.

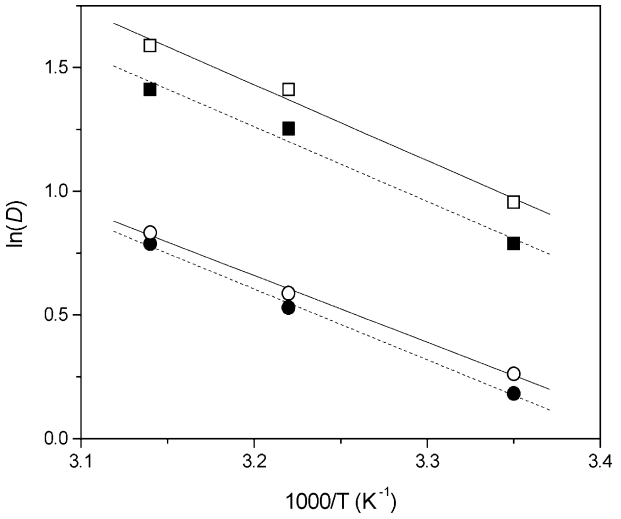

Fig. 5. Arrhenius-type plot of the diffusion coefficients of phosphate in dextran gels. D_s obtained from gels used in release (□) experiments. D_m extracted from release (■), and penetration (types **II** (○) and **III** (●)) experiments.

As expected, the diffusion coefficients increase as the temperature increases. If we plot an Arrhenius-type relation in the form

$$D = D_0 \exp(-E_a/RT), \tag{3}$$

the activation energy (E_a) associated to the diffusion can be calculated (Fig. 5). The resulting activation energies extracted from the slopes are 25 kJ/mol for D_s and D_m derived from release experiments. For the penetration approaches, 22 and 24 kJ/mol were obtained for type **II** and **III** experiments, respectively. Conversely to the diffusion coefficients, E_a values are similar for the microscopic and macroscopic scales, and for the penetration and release experiments. The values that are obtained are comparable with the E_a (18.5–24.5 kJ/mol) reported for various organic solutes in dextran gels (water swollen G-34 Sephadex beads) with similar concentration (about 82% water) [25]. These activation energies in gels are higher than those typically reported for various ions in aqueous solutions, ranging between 16 and 19 kJ/mol [24]. For example, E_a of phosphoric acid in solution is 16.3 kJ/mol [26].

4. Discussion

The main goal of this work was to characterize the micro- and macroscale diffusion of phosphate in hydrogels. NMR experiments were highly suitable as ^{31}P nucleus from the phosphate ion was the only active nucleus in the samples leading to simplified spectroscopy. The diffusion on microscopic scale was characterized using the conventional PFG-SE experiments. The diffusion on macroscopic scale was obtained from 1D ^{31}P NMR profiling, an approach that has not been widely used for this type of applications. In this paper, several 1D-profiles were acquired over a 18-h period to firmly establish the potential of the approach. Over 600 points could be fitted with D_m as a single fitting parameter, using equations derived from Fick's law. Similar values of D_m could indeed be obtained from a single profile. The comparison between mutual- and self-diffusion clearly indicates that macro- and microscopic scale diffusion does not reflect the very same phenomenon in the case of phosphate diffusion in dextran gels, and their differences provide information relative to the structure of the hydrogels.

Although the concentration of the gelifying ion ($[K^+] = 2.5\,M$) was identical, the gels that were used for the release (approach **I**) and the penetration experiments (approaches **II** and **III**) showed actually differences since one contained phosphate ions while the other did not. The introduction of phosphate also resulted in an increase of the proton concentration. The pH of the phosphate-containing solution used to hydrate the gels was 3.7 whereas it was 6.6 for that used to hydrate the phosphate-free gels. The dependence of the gel structure on pH has not been reported. However, it was observed that dextran hardly formed gels in basic K_2HPO_4 solutions (pH 9.0) even when the same amount of gelifying ion ($[K^+] = 2.5\,M$) was present. Consequently, pH might influence the details of the dextran gel structure and such an effect cannot be excluded. In spite of the possible differences in gel structures, D_s values are reproducible for experiments performed at a given temperature. The measurements were performed on systems (i) where phosphate was included in the hydrating buffer or (ii) where a phosphate solution was added in the

reservoir, on top of the gel prepared with a phosphate-free buffer and an appropriate incubation time was allowed to reach equilibrium. No significant difference of D_s could be observed between these two sample preparation approaches, indicating that both approaches likely led to equilibrium.

The D_s value of phosphate free in aqueous solutions ($8.0 \times 10^{-10}\,m^2/s$) is in good agreement with that of $H_2PO_4^-$ in water, at 25 °C, reported to be $9.6 \times 10^{-10}\,m^2/s$ [24]. In most cases, ion self-diffusion decreases as the salt concentration increases [24], and considering that our measurements were performed in a 2.5 M KCl solution, this small decrease is not surprising. The experiments reported here establish that the diffusion of phosphate ions was significantly retarded in the presence of the dextran gels. Self-diffusion coefficients of phosphate in dextran gels are about $3–5 \times 10^{-10}\,m^2/s$, depending on the temperature; the ratio of the diffusion coefficients in dextran gels relative to those in aqueous solutions is about 0.34, indicating a diffusion about three times slower than in the aqueous solutions. This is, to our knowledge, the first report of hindered phosphate diffusion in polysaccharide gels. In a recent paper, the self-diffusion of various neutral molecular solutes in 20% dextran gels was investigated [27]. The ratio of the diffusion coefficients in gels relative to those in dextran-free solutions was between 0.42 and 0.36 for neutral solutes with molecular weight of 46–76. This reduced diffusion is comparable with the behavior reported here for phosphate ions (MW = 97). Dextran is a neutral polymer, and the effect of the charges carried by phosphate ions do not seem to display any special influence on their diffusion in the gels. The restricted diffusion caused by dextran gels would be mainly associated to steric obstacles formed by the polymeric strands.

The different values for D_m and D_s are clearly seen in Fig. 5 and these differences are likely due to time and space sampling differences. For most of our PFG ^{31}P NMR measurements, the diffusion time is about 60 ms. The root mean square distance that a phosphate ion travels during this time is 5.6–7.7 μm. At 25 °C, the diffusion time was increased up to 400 ms. In these conditions, the diffusion scale was about 14 μm. The dependence of the self-diffusion coefficient over the diffusion time has been shown to provide information relative to the pore size in inhomogeneous materials [28–30]. In our case, the results provided no indication of restricted diffusion even for the longest delay. The pore size in our gels is therefore likely larger than the diffusion length associated to the D_s measurements. The pore size in 30% dextran gels with 0.5–2 M K^+ was evaluated to be 8–10 μm [12]. The structure of dextran gels has been shown to depend on both the polysaccharide and K^+ concentrations [12]. Since we have used a lower dextran concentration (20%) and higher potassium ion concentration (2.5 M), the pore size in our systems is expected to be larger than the reported value in [12], and would be consistent with the absence of restricted diffusion concluded from our measurements.

The fact that the pore size is larger than the diffusion length scale is probably at the origin of the slower macroscopic scale diffusion than the microscopic scale one. Mutual-diffusion is expected to be more sensitive to the structure of the gel than the self-diffusion because the diffusing particles should overcome or bypass the barriers formed by the gel to move from one position to the other in the course of the long diffusion length and time. In spite of the significant difference between D_s and D_m, the activation energies related to these two phenomena were similar. This similarity suggests that the diffusion-limiting step is associated to a short distance scale. This step is generally related to breaking the intermolecular interactions with the nearest neighboring molecules [31], a phenomenon that occurs at the molecular level. The slower diffusion observed for the mutual diffusion compared to the self-diffusion can be an indication of the existence of impenetrable obstacles, formed by the polysaccharide network, with a long correlation length (relative to the time scale of D_s measurements). There are only a few reports comparing the micro- and macroscale diffusion on the same systems, in the same conditions. It was previously reported that Laponite clay gels have heterogeneous structures spanning several different length scales from few tens of nanometers to several centimeters [15]. Nonetheless, the similarity of D_s and D_m of water molecules in these gels led to the conclusion that Laponite gels have a very open structure at all length scales. The comparison between that study and our results suggests that the structure of the dextran gels leads to an obstruction effect at a length scale larger than the micrometer, hindering phosphate diffusion. It should be added that phosphate may sense differently the structure of gels since very small solute such as water may not be as sensitive to gel structure, the diffusion of a small probes being found less dependent on the presence of the gel materials than the large ones [32,33]. In fact, D_s values of water measured in clay gels were marginally smaller than that of bulk water while the phosphate ion diffusion was retarded about 3-fold in dextran gels. These considerations indicate that the comparison between self- and mutual-diffusion brings new structural aspects of the gels and such measurements should be encouraged.

In conclusion, we have successfully shown that the 1D ^{31}P NMR profiling approach can define macroscopic diffusion of phosphate in gels. In addition, the presented results ascertain that the microscopic and macroscopic diffusions probe different aspects of the diffusion, because of their different time and spatial scales. The results indicate that phosphate does not diffuse as freely in dextran gels (20%) as in water. This limited diffusion associated to the polysaccharide matrix is a phenome-

non that needs to be examined. For example, this restricted phosphate penetration in this type of matrices may be associated to a lack of nutriments experienced by the bacteria in biofilms that could trigger changes in their physiology [1].

Acknowledgments

This work was supported by NSERC (Canada) and by the FCAR (Québec).

References

[1] G. O'Toole, H.B. Kaplan, R. Kolter, Biofilm formation as microbial development, Annu. Rev. Microbiol. 54 (2000) 49–79.
[2] P. Watnick, R. Kolter, Biofilm, City of microbes, J. Bacteriol. 182 (2000) 2675–2679.
[3] I.W. Sutherland, Biofilm exopolysaccharides: a strong and sticky framework, Microbiology 147 (2001) 3–9.
[4] P.S. Stewart, A review of experimental measurements of effective diffusive permeabilities and effective diffusion coefficients in biofilms, Biotechnol. Bioeng. 59 (1998) 261–272.
[5] P.A. Suci, J.D. Vrany, M.W. Mittelman, Investigation of interactions between antimicrobial agents and bacterial biofilms using attenuated total reflection Fourier transform infrared spectroscopy, Biomaterials 19 (1998) 327–339.
[6] P.A. Suci, G.G. Geesey, B.J. Tyler, Integration of Raman microscopy, differential interference contrast microscopy, and attenuated total reflection Fourier transform infrared spectroscopy to investigate chlorhexidine spatial and temporal distribution in *Candida albicans* biofilms, J. Microbiol. Meth. 46 (2001) 193–208.
[7] J.W. Costerton, P.S. Stewart, E.P. Greenberg, Bacterial biofilms: a common cause of persistent infections, Science 284 (1999) 1318–1322.
[8] A.S. Landa, H.C. Van Der Mei, H.J. Busscher, Detachement of linking film bacteria from enamel surfaces by oral rinses and penetration of sodium lauryl sulfate through an artificial oral biofilm, Adv. Dent. Res. 11 (1997) 528–538.
[9] B.D. Hoyle, J. Alcantara, J.W. Costerton, *Pseudomonas aeruginosa* biofilm as a diffusion barrier to piperacillin, Antimicrob. Agents Chemother. 36 (1992) 2054–2056.
[10] W.B. Neely, Dextran: structure and synthesis, Adv. Carbohydr. Chem. 15 (1960) 341–369.
[11] K. Kajiwara, N. Murase, K. Gonda, Freeze–thawing behavior of saturated saline aqueous solutions in the presence of dextran, Jpn. J. Freezing Drying 33 (1987) 27–31.
[12] T. Watanabe, A. Ohtsuka, N. Murase, P. Barth, K. Gersonde, NMR studies on water and polymer diffusion in dextran gel. Influence of potassium ions on microstructure formation and gelation mechanism, Magn. Reson. Med. 35 (1996) 697–705.
[13] B.A. Westrin, A. Axelsson, G. Zacchi, Diffusion measurement in gels, J. Controlled Rel. 30 (1994) 189–199.
[14] W.S. Price, Pulsed-field gradient nuclear magnetic resonance as a tool for studying translational diffusion: Part I. Basic theory, Concepts Magn. Reson. 9 (1997) 299–336.
[15] F.P. Duval, P. Porion, H. Van Damme, Microscale and macroscale diffusion of water in colloidal gels. A pulsed field gradient and NMR imaging investigation, J. Phys. Chem. B 103 (1999) 5730–5735.
[16] B.J. Balcom, A.E. Fischer, C.T. Adrian, L.D. Hall, Diffusion in aqueous gels. Mutual diffusion coefficients measured by one-dimensional nuclear magnetic resonance imaging, J. Am. Chem. Soc. 115 (1993) 3300–3305.
[17] B. Narasimhan, J.E.M. Snaar, R.W. Bowtell, S. Morgan, C.D. Melia, N.A. Peppas, Magnetic resonance imaging analysis of molecular mobility during dissolution of poly(vinyl alcohol) in water, Macromolecules 32 (1999) 704–710.
[18] T.G. Nunes, G. Guillot, J.M. Bordado, Low-, stray-field imaging and spectroscopic studies of the sodium polyacrylate water uptake, Polymer 41 (2000) 4643–4649.
[19] K.L. Perry, P.J. McDonald, E.W. Randall, K. Zick, Stray field magnetic resonance imaging of the diffusion of acetone into poly(vinyl chloride), Polymer 35 (1994) 2744–2748.
[20] P. Mansfield, R. Bowtell, S. Blackband, Ingress of water into solid nylon 6.6, J. Magn. Reson. 99 (1992) 507–524.
[21] S.L. Talagala, I.J. Lowe, Introduction to magnetic resonance imaging, Concepts Magn. Reson. 3 (1991) 145–159.
[22] J. Crank, The Mathematics of Diffusion, second ed., Clarendon press, Oxford, 1975.
[23] E.O. Stejsksal, J.E. Tanner, Spin diffusion measurements: spin echoes in the presence of a time-dependent field gradient, J. Chem. Phys. 42 (1965) 288–292.
[24] R. Mills, V.M.M. Lobo, Self-diffusion in Electrolyte Solutions: A Critical Examination of Data Compiled from the Literature, Elsevier, Amsterdam, 1989.
[25] S.B. Horowitz, I.R. Fenichel, Solute diffusional specificity in hydrogen-bonding systems, J. Phys. Chem. 68 (1964) 3378–3385.
[26] H.S. Kielman, J.C. Leyte, Selfdiffusion of phosphate and polyphosphate anions in aqueous solution, in: Magnetic Resonance and Related Phenomena, Proceedings of Congress AMPERE, 18th, 1974 vol. 2, 1975, pp. 515–516.
[27] S. Kwak, M. Lafleur, NMR self-diffusion measurements of molecular and macromolecular species in dextran solutions and gels, Macromolecules accepted, 2003.
[28] J.E. Tanner, Transient diffusion in a system partitioned by permeable barriers. Application to NMR measurements with a pulsed field gradient, J. Chem. Phys. 69 (1978) 1748–1754.
[29] E. von Meerwall, R.D. Ferguson, Interpreting pulsed-gradient spin-echo diffusion experiments with permeable membranes, J. Chem. Phys. 74 (1981) 6956–6959.
[30] A. Ohtsuka, T. Watanabe, The network structure of gellan gum hydrogels based on the structural parameters by the analysis of the restricted diffusion of water, Carbohydr. Polym. 30 (1996) 135–140.
[31] R.B. Bird, W.E. Stewart, E.N. Lightfoot, Transport Phenomena, second ed., Wiley, New York, 2002.
[32] B. Amsden, Solute diffusion within hydrogels. Mechanisms and models, Macromolecules 31 (1998) 8232–8395.
[33] A.H. Muhr, J.M.V. Blanshard, Diffusion in gels, Polymer 23 (1982) 1012–1026.